Available online at www.sciencedirect.com
ScienceDirect
Journal of Nuclear Materials 360 (2007) 208–213
journal of nuclear materials
www.elsevier.com/locate/jnucmat

Letter to the Editor

Formation of columnar and equiaxed grains by the reduction of U_3O_8 pellets to UO_{2+x}

Jae Ho Yang [a,*], Young Woo Rhee [a], Ki Won Kang [a], Keon Sik Kim [a], Kun Woo Song [a], Seung Jae Lee [b]

[a] *Advanced LWR Fuel Development, Korea Atomic Energy Research Institute, Deokjin-dong 150, Yuseong-gu, Daejeon-si 305-600, Republic of Korea*

[b] *Nuclear Fuel Design Department, Korea Nuclear Fuel Co., Ltd., P.O. Box 14, Yuseong-gu, Daejeon-si 305-600, Republic of Korea*

Received 3 July 2006; accepted 18 October 2006

Abstract

The reduction of U_3O_8 pellets to UO_{2+x} has been investigated at 1300 °C in H_2, Ar and CO_2 gas atmospheres by TGA, SEM, and X-ray diffraction. The selected U_3O_8 pellet was prepared by sintering a U_3O_8 powder compact. The TGA results show that the reduction rate is fastest in H_2 gas, and X-ray diffraction indicates that U_3O_8 reduces to UO_{2+x} without any intermediate phase. The reduced pellet, UO_{2+x}, has a special grain structure that consists of equiaxed grains at the surface, columnar grains in the middle, and equiaxed grains in the center. The equiaxed grains and columnar grains are much smaller in H_2 gas than in Ar or CO_2 gas. The reducing gases significantly influence the morphology of the grain structure. This difference can be explained in terms of a relation between oxygen potential and critical nucleus size during the reduction.

1. Introduction

The reduction of U_3O_8 to UO_2 has been investigated for a long time. The reduction kinetics is known to depend on the temperature and the gas composition or pressure [1–8]. In addition, the kinetics is also influenced by the powder characteristics such as BET surface area and size [1–4], since the U_3O_8 powder has been used in nearly all the experiments thus far. The reduction reaction occurs in hydrogen gas in the temperature range between 400 and 600 °C. It should be noted that the reduction of U_3O_8 to UO_2 leads to a volume contraction of about 30%, inducing crack formation in the reduced UO_2. This is especially outstanding in reducing bulky U_3O_8 rather than U_3O_8 powder. A high temperature reduction might be needed to accommodate the volume contraction without crack development. Leme and Matzke [9] have measured the U-diffusion coefficient by reducing U_3O_8 pellets in a reducing atmosphere of CO and CO_2 mixture at 800 °C. They found that the reduction did not lead to powder formation. However, detailed microstructure evolution during the reduction of the U_3O_8 pellet in high temperature has not yet been reported.

* Corresponding author. Tel.: +82 42 868 2813; fax: +82 42 861 7340.
E-mail address: yangjh@kaeri.re.kr (J.H. Yang).

0022-3115/$ - see front matter
doi:10.1016/j.jnucmat.2006.10.006

This paper deals with the reduction of pellet-sized U_3O_8 to UO_2 at 1300 °C. In which we found that columnar and equiaxed grains, which are similar to the as-cast microstructure resulting from solidification, are formed in the reduced UO_2 pellet. It is well known that the cast microstructure develops which consists of three different zones of the grain structure [10] while a metal is being solidified. When the melt near the mould surface is under-cooled below its melting temperature, fine crystals are nucleated at the mould surface, forming the chill zone. Then the crystals (grains) grow preferentially into the under-cooled liquid, forming the columnar zone as the heat flows to the mould. In the center of the mould, equiaxed grains are formed. The as-cast structure is common in the liquid–solid phase transformation under a thermal gradient. However, the as-cast like structure can develop in some other cases such as the solid–solid transformation at the interface of a diffusion couple [11] or the gas–solid transformation during a thin solid film fabrication [12].

This paper shows that the as-cast like structure can be developed by reducing a U_3O_8 pellet to UO_2 at high temperature. This paper also describes the grain structure evolution during the reduction experiments in various reducing gases with different oxygen partial pressures.

2. Experimental

The U_3O_8 powder was obtained by oxidation of ADU-UO_2 powder at 400 °C in air. The U_3O_8 phase formation was identified by X-ray diffraction. The green pellet samples of U_3O_8 were prepared by pressing the U_3O_8 powder under a pressure of 3 t/cm^2. Upon heating of the green pellet to 1300 °C at a rate of 5 K/min in air, it was sintered to a dense U_3O_{8-x} pellet. When the temperature of the specimen reached 1300 °C, the isothermal reduction of the U_3O_{8-x} pellets was conducted in the reducing gas atmospheres of H_2, Ar and CO_2, respectively. The oxygen potential of each reducing gas was calculated with the HSC program [13]. Table 1 provides the impurity contents in the reducing gases and corresponding calculated oxygen potential at 1300 °C together with the equilibrium oxygen potentials for the uranium oxides with different O/U ratios [14,15]. The weight loss during the isothermal reduction was continuously measured by the thermogravimetric analysis (TGA, TG-51 Shimadzu). The microstructure of the UO_2 pellet produced by the TGA experiments was examined by an optical microscope and SEM. The polished section of the sintered pellets and the mechanically fractured sample were prepared for an optical microscope and SEM, respectively. The phase evolution was characterized in accordance with the degree of reduction by the X-ray diffraction profiles.

3. Results

A green pellet of U_3O_8 was sintered at 1300 °C for 10 min in air. The heating and cooling rate was 5 K/min. The O/U ratio change during the sintering was monitored by the TGA. U_3O_8 is known to loose oxygen on annealing in air at temperature above ~700 °C [16,17]. The present sample also continuously looses its weight upon heating to 1300 °C. The composition at the 1300 °C was calculated to be $UO_{2.593}$. When the sample was cooled to room temperature, the sample weight slightly increased and the final composition of an as-sintered pellet was calculated to be $UO_{2.61}$. The average density of pellets, measured at room temperature, was 8.19 g/cm^3. This is about 97.5% of the theoretical density of U_3O_8. Fig. 1 shows the SEM image of the grain structure at the

Table 1
The equilibrium oxygen potentials of the reducing gases and uranium oxides

Species	Impurity contents (ppm)						Equilibrium oxygen potential at 1300 °C (kJ/mol)
	O_2	H_2O	CO_2	N_2	Ar	CO	
H_2	1	1	0.1	–	–	–	−591.1 [13]
Ar	1	1	0.1	–	–	–	−149.2 [13]
CO_2	3	10	–	50	7	10	−97[a]
$U_3O_{7.83}$							−59.03 [15]
$UO_{2.20}$							−111.9 [15]
$UO_{2.0001}$							−386 [15]

[a] Oxygen potential of CO_2 gas was measured by an oxygen sensor.

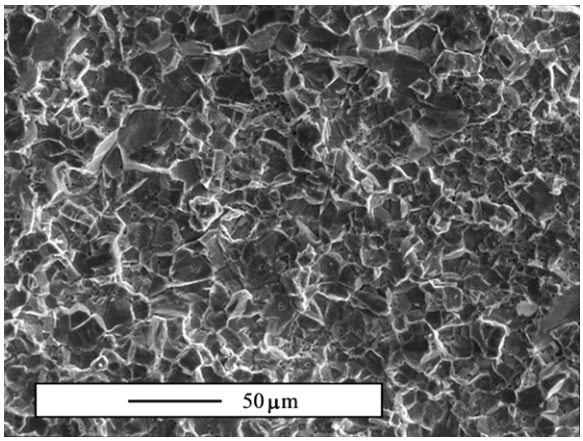

Fig. 1. Fractography of the grains from the sintered U_3O_{8-x} pellet.

fractured surface of a U_3O_{8-x} sintered pellet and this has a normal grain structure.

The U_3O_8 green pellet was heated to 1300 °C at a rate of 5 K/min in air and held there for a few minutes. And then it was isothermally reduced in a H_2 atmosphere. Fig. 2 shows the SEM micrograph of the grain morphology at the fractured surface of a reduced sample pellet. The photo of the center shows the complete microstructure of the pellet. Magnified images from different positions in the pellet are also shown in Fig. 2(a)–(d). The grain structure of the reduced pellet is quite different from that of the U_3O_{8-x} pellet shown in Fig. 1. At the periphery of the pellet (see Fig. 2(c)), the layer consisting of equiaxed grains is formed. Inside of this layer, the grains grow into the pellet center and form a columnar grain structure (see Fig. 2(d)). In the center, Fig. 2(a), fine and equiaxed grains are developed. These overall features closely resemble the as-cast structure formed during the solidification of liquid under thermal gradient. It is the key finding of this work that the as-cast structure develops during a solid-state reduction of the U_3O_{8-x} pellet.

Fig. 2 shows various sized cracks in the reduced pellet. It is well known that the reduction of U_3O_8 to UO_2 leads to a large volume contraction [18]. Once the UO_2 phase at the periphery forms a rigid shell, the volume contraction in the inner pellet cannot be accommodated without inside cracks. The inner equiaxed zone is porous, probably because the volume contraction is uniformly accommodated in it. However, the columnar zone seems to be dense and nearly free of cracks, but the large circumferential crack is formed at the end of the columnar zone. It is supposed that the columnar grain structure is

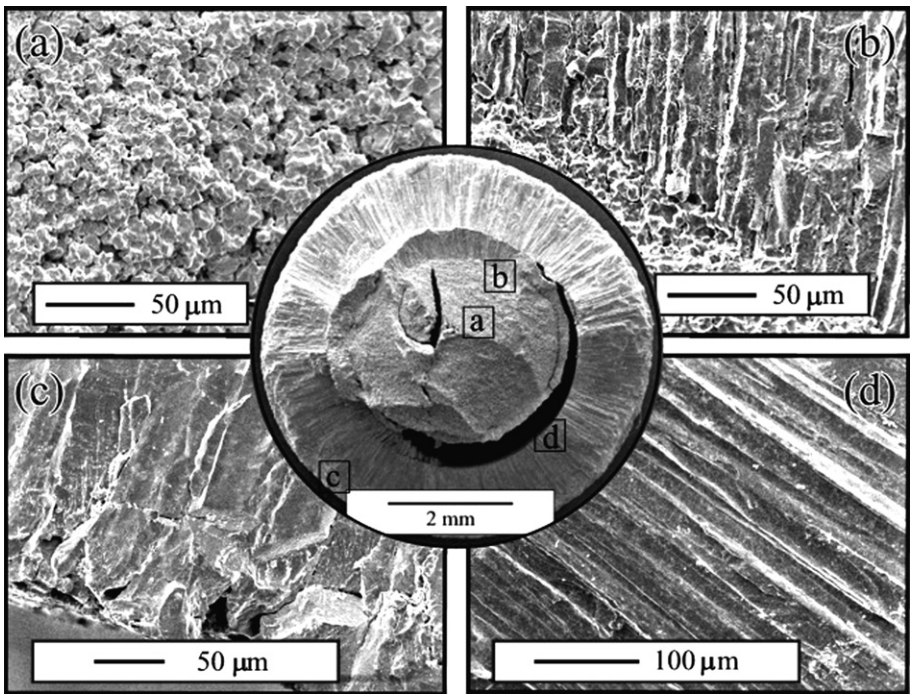

Fig. 2. The SEM images from the fractured surface of a pellet obtained by reducing the U_3O_8 sintered pellet at 1300 °C in H_2 atmosphere. The photo in the center represents the whole image. (a)–(d) Enlarged images from the position denoted in the central photo.

resistant to crack formation, and that the large circumferential crack is produced by the volume contraction associated with the columnar zone.

Fig. 3(a)–(c) shows the XRD patterns of three sample pellets: before reduction, 50 min reduction, and after complete reduction. The reaction condition was at 1300 °C in the Ar gas atmosphere. The XRD profiles were collected at room temperature from the sample pellets after the reaction. A full pattern analysis of the X-ray data measured for the pellet before reduction (Fig. 3(a)) shows that the structure is orthorhombic with a unit cell of $a = 4.134(1)$Å, $b = 11.856(3)$Å and $c = 6.720(2)$Å. The lattice parameter and relative integral peak intensity closely resemble those of α-U_3O_8 (Amm2) [19–23]. The calculated unit cell parameter, however, is different from that of stoichiometric U_3O_8. c is increased and b is decreased. This deviation is known to occur in the hypostoichiometic U_3O_{8-x} [24] and it is in good agreement with the TGA results. When the sample is annealed at 1300 °C in Ar for 50 min, Fig. 3(b), diffraction lines from the cubic UO_{2+x} phase appeared together with those from U_3O_{8-x}. When the reaction is finished, Fig. 3(c), the U_3O_{8-x} phase disappeared and the diffraction pattern showed typical diffraction lines of the cubic UO_2 phase. The calculated lattice parameter of a reduced phase is 5.4460(5)Å. This is smaller than that of stoichiometric UO_2. The lattice parameter of UO_{2+x} is known to decrease with increasing the O/U ratio. According to the literature, the O/U ratio of the present sample is about 2.2 [25]. The XRD pattern evolution according to the reaction time indicates that the U_3O_{8-x} pellet is reduced directly to UO_{2+x} without any intermediate phase, suggesting that the reduction of U_3O_8 proceeds by the nucleation and growth of the cubic UO_{2+x} phase in the U_3O_{8-x} matrix [3].

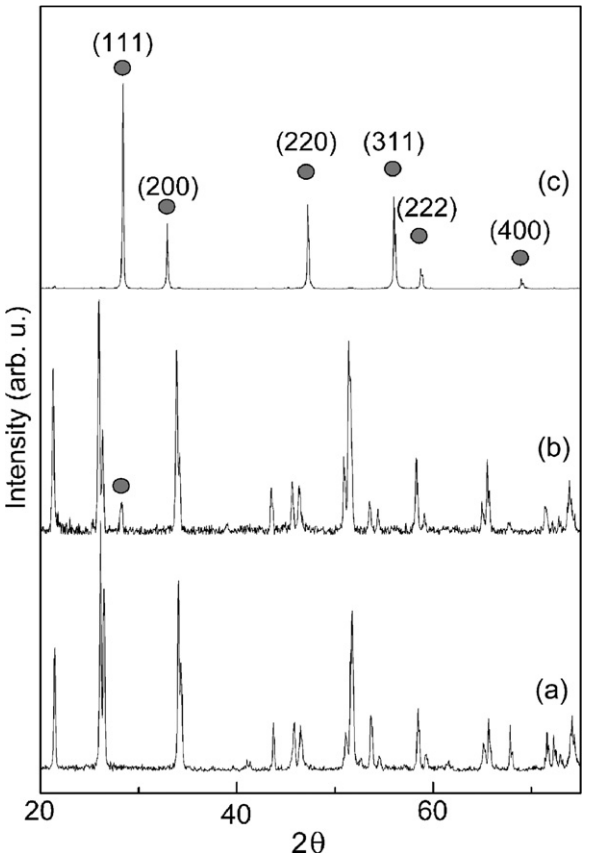

Fig. 3. X-ray diffraction profiles from the longitudinal sections of the pellet (a) before reduction, (b) 50 min reduction, and (c) after complete reduction in Ar at 1300 °C.

In order to examine the influence of the oxygen potential of the reducing gas atmospheres on the reduction kinetics and microstructure evolution of U_3O_8 pellet, three different gases, H_2, Ar and CO_2, have been used for the reducing gases. As shown in Table 1, the oxygen potential of the reducing gases at 1300 °C is lower than that of the U_3O_{8-x} phases, making it possible to reduce the U_3O_{8-x} phase to the UO_{2+x} phase at 1300 °C. The oxygen potential difference is different for each gas: It is much higher in H_2 than in Ar or CO_2.

The reduction kinetics of the U_3O_8 pellet under different reducing gases was observed through the TGA experiment. The U_3O_8 green pellets were heated up to 1300 °C in air, and then the appropriate reducing gas was provided under isothermal conditions of 1300 °C. Fig. 4 shows the curves of the weight loss of the U_3O_8 pellets. The arrows in the figure indicate the times when the reducing gases

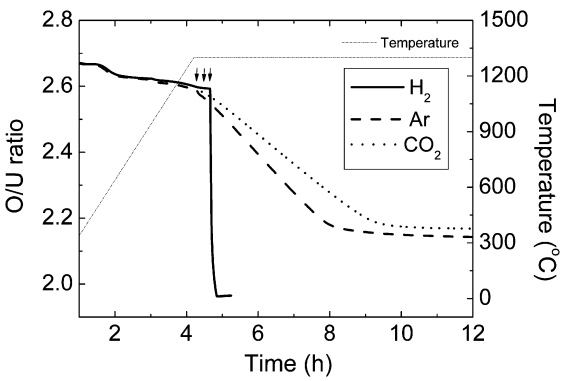

Fig. 4. TGA reduction-kinetics curves of the U_3O_8 pellet to UO_2 according to the reducing gas atmospheres.

were supplied. During the ramping to 1300 °C under air, the U_3O_8 pellet loses its weight slightly. This corresponds to the reduction of U_3O_8 to U_3O_{8-x} [9,15]. By isothermal annealing at 1300 °C, the sample weight is continuously decreased with the holding time. As the weight loss is attributed to the reduction of the U_3O_{8-x} phase to UO_{2+x}, the kinetics of the weight loss can be regarded as that of the reduction. Fig. 4 shows that the reduction reaction is much faster in H_2 than in Ar or CO_2.

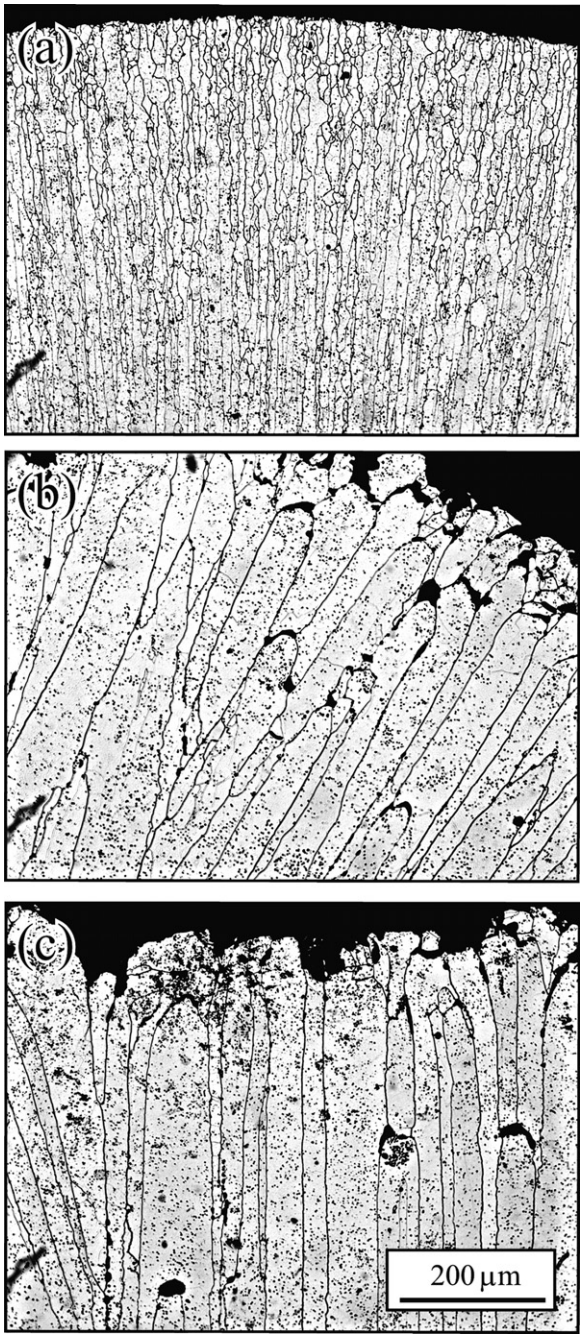

Fig. 5. Optical microstructure at the chill and columnar zones of the reduced pellets. (a) H_2, (b) Ar, (c) CO_2.

The samples after the TGA experiment were polished and thermally etched for an optical microscopy investigation. Fig. 5 shows the optical micrographs of the reduced pellets. It can be readily seen that the equiaxed grains at the surface and the columnar grains at the interior are quite different depending on the reducing gases. In the pellet reduced in H_2, the equiaxed grain is very small when compared to that in the other gases. The equiaxed grain size seems to be consistent with the width of columnar grains, which suggests that the UO_2 grains are formed in a random orientation at the surface and then certain favorably-oriented grains at the UO_2/U_3O_8 interface begin to grow inward. The columnar grains grow directionally and the interface between two adjacent columnar grains is almost flat. The columnar grain size is small in H_2, while the columnar grain size of the pellets reduced in CO_2 and Ar becomes large at up to 100 μm wide and 1000 μm long.

4. Discussion

Experimental results show that the reducing gases greatly influence the grain structure. The reducing gas, in principle, determines the magnitude of oxygen potential difference. It is well known that the critical nucleus size becomes smaller with increasing the free energy difference when the nucleation and growth mechanism governs the phase transformation, for example, the solidification by under-cooling of liquid. The critical nucleus size predominantly determines the grain size of equiaxed grain at the surface.

The released oxygen at the U_3O_8/UO_{2+x} interface has to diffuse out through the UO_{2+x} zone to the environment, and thereby, an oxygen potential gradient is created in the UO_{2+x} zone. When the thickness of the UO_{2+x} (equiaxed grain) zone increases to such an extent that dissociated oxygen atoms are not sufficiently diffused out, the oxygen potential of UO_{2+x} at the U_3O_8/UO_{2+x} interface is likely to increase, while the oxygen potential of UO_{2+x} remains unchanged at the surface in contact with the gas environment. This induces a decrease in oxygen potential difference between U_3O_8 and UO_{2+x} at the interface, so crystal nucleation is no longer dominant and the reduction condition becomes more favorable for crystal growth. In this

situation, certain favorably oriented crystals at the U_3O_8/UO_2 interface begin to grow into the center, forming a columnar grain structure. At this point, the columnar grain width should be consistent with the equiaxed grain size near the surface. That is, the columnar grain width also depends on the critical nucleus size. Fig. 5 shows that the columnar grain width is much narrower in H_2 gas than in Ar or CO_2 gas, which also reflects well that the critical nucleus size of the UO_{2+x} phase is much smaller in H_2 gas.

The experimental result that the grain structure is dependent on the oxygen potential of the reducing gas atmosphere has made it possible to tailor the grain size or grain texture of the UO_2 pellet simply by changing the oxygen partial pressure of the reducing gas atmosphere. This method has a potential for applications such as the fabrication of a single crystal UO_2 or textured UO_2 pellet etc. [26–28].

5. Conclusion

When the U_3O_8 pellet is reduced to UO_{2+x} at 1300 °C in H_2, Ar, and CO_2 atmospheres, a special grain structure develops in the UO_{2+x} pellet which consists of equiaxed grains at the surface, columnar grains in the middle, and equiaxed grains in the center. In a H_2 gas atmosphere, the equiaxed grains at the surface and in the middle of columnar grains are much smaller than in Ar or CO_2 gas. This experimental result can be interpreted by the fact that H_2 gas provides much larger oxygen potential difference for U_3O_8 than Ar or CO_2 gas. It can be concluded that the oxygen potential of reducing gas controls the nucleation rate and nucleus size of UO_{2+x} when the U_3O_8 pellet is reduced to UO_{2+x}.

Acknowledgement

This study has been carried out under the Nuclear R&D Program by MOST (Ministry of Science and Technology) in Korea.

References

[1] A.H. Le Page, A.G. Fane, J. Inorg. Nucl. Chem. 36 (1974) 87.
[2] M. Pijolat, C. Brun, F. Valdivieso, M. Soustelle, Solid State Ionics 101–103 (1997) 931.
[3] C. Burn, F. Valdivieso, M. Pijolat, M. Soustelle, Phys. Chem. Chem. Phys. 1 (1999) 471.
[4] F. Valdivieso, M. Pijolat, M. Soustelle, J. Jourde, Solid State Ionics 141&142 (2001) 117.
[5] H. Chevrel, P. Dehaudt, B. Francois, J.F. Baumard, J. Nucl. Mater. 189 (1992) 175.
[6] K.W. Song, K.S. Kim, K.W. Kang, Y.H. Jung, J. Nucl. Mater. 279 (2000) 356.
[7] K.W. Song, K.S. Kim, K.W. Kang, Y.M. Kim, J.H. Yang, Y.H. Jung, J. Kor. Nucl. Soc. 31 (1999) 455.
[8] M.S. Yang, H.B. Choi, C.J. Jeong, K.C. Song, J.W. Lee, G.I. Park, H.D. Kim, W.I. Ko, J.J. Park, K.H. Kim, H.H. Lee, J.H. Park, Nucl. Eng. Technol. 38 (2006) 361.
[9] D.G. Leme, Hj. Matzke, J. Nucl. Mater. 115 (1983) 350.
[10] H. Biloni, W.J. Boettinger, in: R.W. Cahn, P. Haasen (Eds.), Physical Metallurgy, 4th Ed., North-Holland Physics, Amsterdam, 1996, p. 669.
[11] V. Buscaglia, F. Caracciolo, B. Bottino, M. Leoni, P. Nanni, Acta Mater. 45 (1997) 1213.
[12] M. Ohring, The Materials Science of Thin Films, Academic, 2001, 386.
[13] A. Roine, Outokumpu HSC Chemistry for Windows, Ver. 5.1, 2002, Outokumpu Research Oy: Pori, Finland.
[14] D. Labroche, O. Dugne, C. Chatillon, J. Nucl. Mater. 312 (2003) 21.
[15] Y.S. Kim, J. Nucl. Mater. 279 (2000) 173.
[16] J. Belle (Ed.), Uranium Dioxide, Properties and Nuclear Application, USA Washington, DC, 1961.
[17] T. Fusino, H. Tagawa, T. Adachi, J. Nucl. Mater. 97 (1981) 93.
[18] K.W. Song, M.S. Yang, J. Nucl. Mater. 209 (1994) 270.
[19] S. Siegel, Acta Cryst. 8 (1955) 617.
[20] B.O. Loopstra, Acta Cryst. 17 (1964) 651.
[21] R. Herak, Acta Cryst. B 25 (1969) 2505.
[22] B.O. Loopstra, J. Appl. Cryst. 3 (1970) 94.
[23] B.O. Loopstra, Acta Cryst. B 26 (1970) 656.
[24] R.J. Ackermann, A.T. Chang, C.A. Sorrell, J. Inorg. Nucl. Chem. 39 (1977) 75.
[25] B. Belbeoch, E. Laredo, P. Perio, J. Nucl. Mater. 13 (1964) 100.
[26] D. Kolberg, F. Wastin, J. Rebizant, P. Boulet, G.H. Lander, J. Schoenes, Phys. Rev. B 66 (2002) 214418.
[27] M.R. Castell, Phys. Rev. B 68 (2003) 235411.
[28] Z. Shen, J. Liu, J. Grins, M. Nygren, P. Wang, Y. Kan, H. Yan, U. Sutter, Adv. Mater. 17 (2005) 676.